High Energy, Sub-Cycle, Field Synthesizers

Haochuan Wang, Ayman Alismail, Gaia Barbiero, Raja Naeem Ahmad, and Hanieh Fattahi

(Invited Paper)

***Abstract*—Tailoring the electromagnetic field transients has been a prominent research focus over the last decade. Advances in ultrashort pulse generation and stabilizing the carrier phase of the electromagnetic field relative to its envelope allowed for extension of coherent synthesis to optical frequencies and ultrashort pulse domain at tens of microjoules of energy. In parallel, ytterbium-doped lasers become a mature technology. They are able to deliver down to 1-picosecond scale pulses at hundreds of millijoule energy and kilowatt-scale average power, making them suitable frontends for scaling the energy and power of light transients. In this paper, we discuss two conceptual schemes, our experimental results, and technological challenges for generation of sub-cycle light transients based on Yb:YAG thin-disk lasers by direct and efficient spectral broadening of ytterbium-doped lasers, and by coherent combination of pulses from multiple broadband optical parametric amplifiers. Moreover, a conceptual design study for a novel synthesis scheme based on polarization splitting of a broadband spectrum and amplification of each polarization in a separate stage is presented. The novel sources hold promise for studying and controlling the nonlinear interactions of matter with custom-tailored light transients at a sub-cycle period of their electric field, opening up unprecedented opportunities in attoscience and strong-field physics.**

***Index Terms*—Ultrabroadband sources, parametric amplifiers, pulse synthesis, waveform nonlinear optics, high harmonic generation, Yb:YAG thin-disk laser.**

I. Introduction

SINCE the invention of laser, ever shorter pulses are generated by temporal shaping and accurate control of the dispersion of the light in sub-cycle regime. These advance, combined with optimized spatial localization of light in nanoscopic volumes [1], [2], could pave the way in electronic signal processing to higher clock rates and ultimately up to optical frequencies [3]–[5]. Moreover, the ability to accurately control the temporal profile of light is crucial and advantageous for high-energy coherent control and high field processes [6].

Three parameters define the time dependence of the electromagnetic field and its temporal shape: i) spectral bandwidth according to Fourier theory, ii) relative spectral intensity of the present frequency components, and iii) spectral phase. Ultrashort pulse shaping in the picosecond (ps) and down to sub-ten femtosecond (fs) scales have been demonstrated by employing various methods such as: prisms, gratings, dispersive mirrors [7]–[9], spatial light modulators [10], [11] or acousto-optic programmable dispersive filters [12]. These techniques allow for tuning the spectral phase and for the two latter cases also the amplitude of a pulse. The flexibility enables crafting a desired field transient, within the limit imposed by the bandwidth. However, all the mentioned techniques are limited in terms of either the spectral bandwidth or the pulse energy, or both.

In 2011, short-pulse generation and pulse shaping entered the new regime of sub-cycle control at microjoule (μJ) energies [13]. It is shown that a μJ-level, super-octave spectrum generated from a gas-filled hollow-core fiber can be compressed to its Fourier limit by coherent electric field synthesis [14]. In this approach the broadband spectrum is decomposed into several spectral regions. Each spectral region is compressed to its Fourier transform limit by using a chirped-mirror compressor. Finally all the channels are coherently superimposed interferometrically to create sub-cycle light transients. The ultimate shape of such light transients are defined by the relative temporal delay of the electric field and the relative spectral intensity of each channel. Therefore, the carrier-to-envelope phase (CEP) stability [15] of the input pulses to such an interferometer is crucial. Nowadays light transients at μJ-level energy and sub-ten kilohertz (kHz) repetition rates can be generated routinely in the laboratories. They provide unprecedented flexibility for not only steering lightmatter interactions but also on triggering and probing electron dynamics with sub-fs precision [16], [17]. However, they are limited in peak- and average-power. Coherent combination of pulses from multiple broadband optical parametric amplifiers (OPA) holds promise for overcoming these limitations and for generation of light transients with higher peak- and average-power [18]–[20].

In what follows we explore possible routes for generation of light transients at higher energy and average-power. Our focus

Manuscript received January 21, 2019; revised April 11, 2019; accepted June 10, 2019. Date of publication June 20, 2019; date of current version July 18, 2019. The work of H. Fattahi was supported by MINERVA scholarship of Max Planck Society. *(Haochuan Wang and Ayman Alismail are first co-authors.) (Corresponding author: Hanieh Fattahi.)*

H. Wang is with the Max-Planck-Institut für Quantenoptik, D-85748 Garching, Germany, and also with the Fakultät für Physik, Ludwig-Maximilians-Universität München, D-85748 Garching, Germany (e-mail: haochuan.wang@mpq.mpg.de).

A. Alismail is with the Fakultät für Physik, Ludwig-Maximilians-Universität München, D-85748 Garching, Germany, and also with the Department of Physics and Astronomy, King Saud University, Riyadh 11451, Saudi Arabia (e-mail: ayman.alismail@physik.uni-muenchen.de).

G. Barbiero is with the Max-Planck-Institut für Quantenoptik, D-85748 Garching, Germany, and also with the Fakultät für Physik, Ludwig-Maximilians-Universität München, D-85748 Garching, Germany (e-mail: gaia.barbiero@mpq.mpg.de).

R. N. Ahmad is with the Fakultät für Physik, Ludwig-Maximilians-Universität München, D-85748 Garching, Germany (e-mail: ahmad.naeem@physik.uni-muenchen.de).

H. Fattahi is with the Max-Planck-Institut für Quantenoptik, Hans-Kopfermann-Str.1, D-85748 Garching, Germany (e-mail: hanieh.fattahi@mpq.mpg.de).

Color versions of one or more of the figures in this paper are available online at http://ieeexplore.ieee.org.

Digital Object Identifier 10.1109/JSTQE.2019.2924151

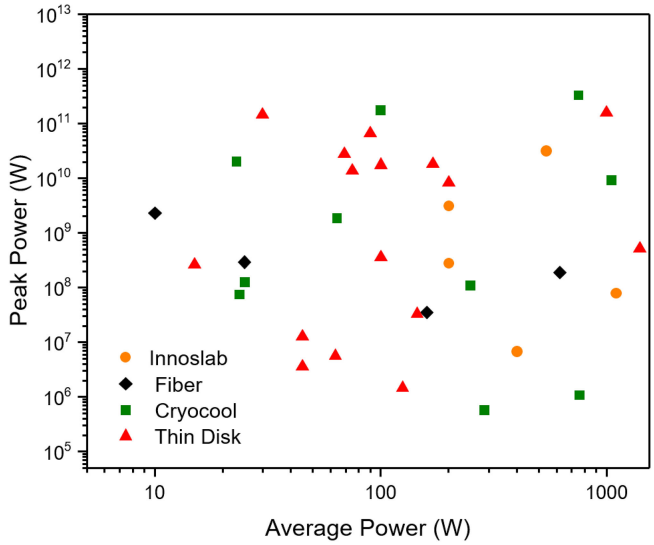

Fig. 1. Summary of the recorded performances of Yb-doped lasers in four different geometries in terms of average and peak powers. The orange dots show the performance of Yb:YAG Innoslab lasers corresponding to Refs. [22]–[26]. The purple dots demonstrate Yb:YAG fiber lasers corresponding to [27]–[30]. The green dots represent the Yb:YAG cryo-cooled sources [31]–[41]. The performance of the Yb:YAG thin-disk lasers are demonstrated by red dots [42]–[57].

is on schemes which allow for temporal shaping of light transients. For a review of other methods of short-pulse generation or spectral shaping, the interested readers are kindly referred to [19], [21].

II. Field Synthesizers Based on Yb-Doped Sources

Nowadays, Yb-doped lasers in fiber, thin-disk, or slab geometries are capable of delivering pulses at variety of energies and repetition rates (see Fig. 1). However, their narrow-band emission cross-section [58] in addition to the gain narrowing limits their pulse duration to tens of ps at J and hundreds of fs at μJ energy.

As can be seen in Fig. 1, the performance of Yb:YAG thin-disk lasers, spans a wide range of average powers with a relatively higher peak power compared to the other technologies. The simultaneous energy and average-power scaling is due to the efficient heat removal from the gain medium, as the gain medium typically consists of a 100 μm-thick Yb:YAG disk mounted on a water-cooled diamond substrate. The efficient cooling allows for high pump power densities exceeding 5 kW/cm^2. However, single-pass gain in disk-geometry is relatively low and typically in the order of 10% (small signal), which is compensated by multiple passes through the gain medium or serial combination of several disks [49].

These unique properties, in combination with the reliability of industrial diode pumps, makes Yb:YAG lasers potential drivers for high-energy, high-average power light transients. Two approaches can be employed to expand the spectral bandwidth of the high-energy and/or high-power pulses: i) direct, efficient spectral broadening, or ii) optical parametric amplification, which are discussed in details in II-A and II-B.

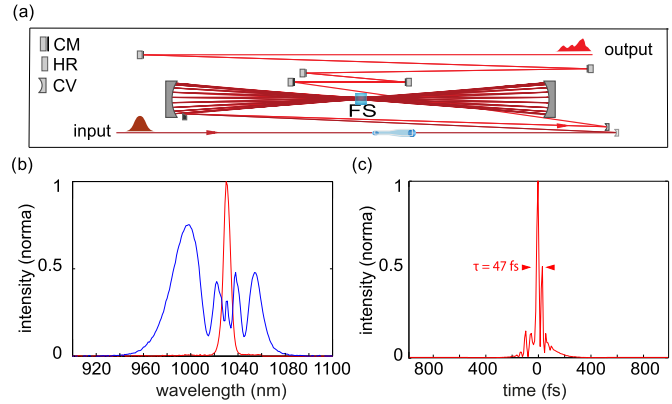

Fig. 2. a) Scheme of the multi-pass cell setup and the additional chirped-mirror compressor (top view). b) Measured input (red) and output (blue) spectra. c) Temporal profile of the compressed pulse, retrieved from a second harmonic FROG measurement. The arrows mark the full width at half maximum (FWHM) pulse duration of the compressed pulses. FS: fused silica, CM: chirped mirror, HR: high reflective mirror, CV: concave mirror.

A. Direct, Efficient Spectral Broadening

Third-order nonlinear processes and in particular, self-phase modulation (SPM) has been one of the common methods for spectral broadening [59], [60]. In SPM, an induced nonlinear phase results in the generation of new frequencies. The nonlinear phase is proportional to the laser intensity, nonlinear refractive index, and the length of the nonlinear medium. Therefore, SPM in free space results in distortion and inhomogeneous spectral broadening in a beam with a Gaussian transverse profile.

In 2016, Schulte *et al.* [61] proposed a new concept to overcome the spatial inhomogeneity and the poor optical-to-optical conversion efficiency. In this concept the beam propagates through a nonlinear medium, in a geometry similar to an optical cavity. In each round trip the nonlinear phase shift is kept below 0.1 rad. The accumulated nonlinear phase shift defines the ultimate spectral bandwidth, while only the fundamental spatial mode survives in the optical cavity geometry. Based on this technique, 10-fold spectral broadening, 5-fold temporal compression and more than 90% optical-to-optical efficiency was demonstrated [61]–[63]. Incorporating a Herriot-cell with the resonator stability condition around the nonlinear medium allows for more than 50 passes through the nonlinear medium in a table-top setup [62].

Fig. 2 a) shows the scheme of a high-power, multi-pass spectral broadening system developed by Barbiero *et al.* [64]. 6 μJ, 265 fs pulses of an Yb:YAG thin-disk laser operating at 16 MHz repetition rates are sent to a multi-pass Herriot-cell containing a 6.3 mm-thick fused silica. The cell incorporates high reflective dispersive mirrors to compensate for the chirp that the pulse acquires in each pass through the crystal. After 34 passes, a 11.3-fold spectral broadening with the 78% optical-to-optical conversion efficiency is achieved. The residual dispersion on the output pulses is compensated by using 6 additional broadband dispersive mirrors to 47 fs pulse duration at full width at half maximum (FWHM). Fig. 2 b) and c) show the initial and broadened spectra, and the reconstructed temporal profile of the output pulses

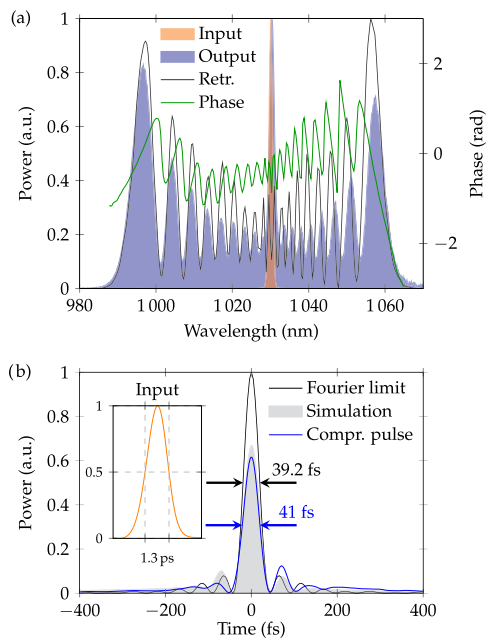

Fig. 3. a) Measured input (orange) and output (blue) spectra of the multi-pass cell. Additionally depicted are the retrieved spectrum (black) and phase (green) from the SHG-FROG measurement of the compressed pulse. b) Blue curve shows the measured compressed pulses after the multi-pass cell using chirp-mirror compressor and the black curve presents its Fourier transform limit. The gray area shows the simulation of the nonlinear compression. The arrows mark the FWHM duration of the compressed pulse (blue) and the Fourier-limited pulse (black). The measured input pulse and its FWHM duration are shown in the inset [66].

after the final compression from a second harmonic generation frequency-resolved optical gating (SHG-FROG) measurement. By implementing additional multi-pass cells, sub-20 fs pulses have been demonstrated [65].

In 2018 Kaumanns *et al.* [66] showed the energy scalability of this approach to higher pulse energies by replacing the nonlinear medium with low-pressure noble gas. The authors could demonstrate the partial compression of the energy delivered by a 200 mJ, 5 kHz Yb:YAG thin-disk regenerative amplifier [49] to 41 fs (Fig. 3). The compression was limited to 18 mJ pulses due to ionization of the noble gas or the damage of the multi-pass mirrors. However, using a longer cavity could allow for energy scaling up to 100 mJ.

The described spectral broadening processes maintain the CEP-stability of the input pulses. Despite many attempts [67]–[70], CEP-stability of Yb:YAG laser sources has been demonstrated only over less than one minute time interval. These powerful and efficient sources can be directly used as the driver of a field synthesizer, if their CEP-stability were improved and their pulse duration reduced. But for the time being, OPAs are the current method of choice for high-energy, high-power, multi-octave filed synthesis.

B. Optical Parametric Amplification

OPA is a popular method for scaling the energy and average power of few-cycle pulses [46], [71]–[74]. Here, unlike stimulated emission, the carrier frequency of the amplified spectrum is not limited to the gain medium. In the presence of powerful pump pulses and by exploiting the second-order nonlinearity of materials and by fulfilling the phase matching condition, the energy of broadband seed pulses can be amplified at different carrier frequencies. The phase-matching condition can be fulfilled in different schemes like: non-collinear OPA (NOPA) [75], [76], degenerate OPA (DOPA) [77], or frequiency domain OPA (FOPA) [78]. In degenerate OPAs, the gain medium has zero group delay dispersion at the carrier frequency of the idler and signal pulses and enables a broadband gain. However, in this case, the second harmonic generation of the broadband signal is also phase-matched which results in an unwanted backward flow of energy from signal to the pump pulses, limiting the optical-to-optical conversion efficiency. For frequencies away from the zero group delay dispersion, the phase-matching condition is fulfilled by inducing geometrical delay to achieve a broadband amplification (NOPA).

Despite the low conversion efficiency of broadband OPAs in the order of 10–30%, they are a desired approach for generating short pulses due to their: i) broadband amplification gain in various central frequencies from ultra-violet (UV) to mid-infrared (MIR) [77], [79]–[82], ii) preservation of the CEP, iii) scalability in power and energy, and iv) simplicity. The key ingredients for OPAs as a driver for high-energy field synthesizers are turn-key, powerful pump, and CEP-stable, super-octave seed pulses. As we discussed earlier in this section, Yb-doped lasers have started to satisfy these criteria. In what follows we briefly discuss the current status of Yb:YAG thin-disk lasers for pumping OPAs (see II-B1), different possibilities for the generation of CEP-stable, super-octave OPA seed pulses (II-B2), details of a three channel optical parametric amplifier and its coherent synthesis (II-B3), and the simulated high harmonic spectra driven by the synthesized waveforms (II-B4).

1) Yb:YAG Thin-Disk Amplifiers: In OPA the duration of the pump pulse and its optimum spatio-temporal overlap with seed pulse has an important role in the amplification process. One the one hand, the damage threshold intensity for transparent materials is proportional to the inverse square root of the pulse duration. On the other hand, the impact of the temporal walk-off between pump and seed pulses scales inversely with their pulse duration. In addition, for optimum energy extraction and conversion efficiency the seed pulses should be stretched within the temporal profile of the pump pulses in a scheme called optical parametric chirped pulse amplification (OPCPA). Employing short pulses to pump an OPCPA simplifies the temporal stretching and recompression of seed pulses. These effects place opposing demands on the pump pulse duration.

Fig. 4 shows the simulated OPCPAs with similar parameters except different pump pulse durations (simulation parameters are summarized in Table I). The amplified spectra are shown in Fig. 4a). As the seed pulses have a linear positive chirp, the center of mass of the amplified spectrum moves towards the longer wavelengths for short pump pulse duration. This is due to the temporal walk-off between pump and seed pulses and the overlap of the leading edge of the seed pulses with the undepleted region of the pump pulses. It can be seen that the amplified peak

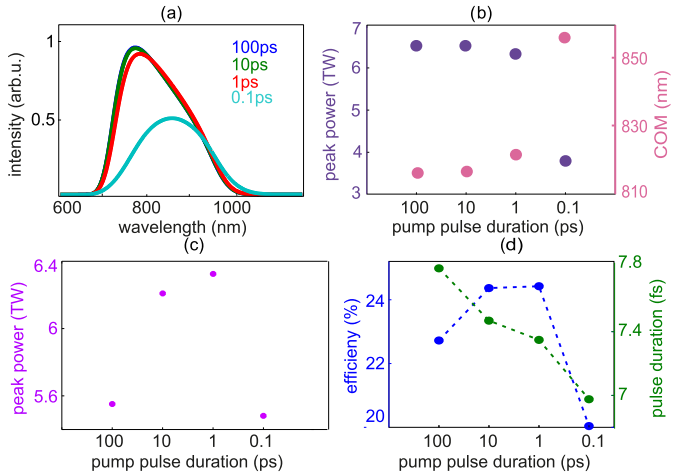

Fig. 4. Simulated amplification performance for OPCPAs with different pump pulse durations and similar pump peak intensity: a) amplified spectra for different pump pulse durations in a saturated OPCPA. The amplified spectra of 10 ps and 100 ps pump pulses are overlapped. b) Peak power of the amplified signal and the corresponding center of mass (COM) versus pump pulse duration. Simulated amplification performance for OPCPAs with different pump pulse durations and pump peak intensities scaled to the corresponding damage threshold: c) peak power of the amplified signal. d) Pump-to-signal conversion efficiency and the amplified signal pulse duration of OPCPAs with different pump pulse durations [83].

TABLE I
SIMULATION PARAMETERS FOR THE CURVES SHOWN IN FIG. 4

Crystal	d_{eff}	E_{seed} / E_{pump}	Pump		Seed	
			space	time	space	time
BBO	2.3168 pm/V	3×10^{-3}	Gaussian	Gaussian	Gaussian	4th order Gaussian linearly chirped

power drops for 100 fs pump pulses due to the temporal walk-off between the pump and seed pulses (see Fig. 4b)).

Fig. 4 c) and d) show the peak power of the amplified signal, pump-to-signal conversion efficiency, and the amplified signal pulse duration of OPCPAs with different pump pulse durations. For each case the pump intensity was adjusted to below the damage threshold intensity in the crystal and accordingly the length of the crystal was modified to reach saturation. As can be seen, pump pulses at around 1 ps appear as the best compromise, which are delivered nowadays by diode-pumped Yb:YAG thin-disk lasers. Short pump pulses allow a higher peak intensity on the nonlinear medium which makes it possible to achieve the required gain in a shorter medium. This results in a greater amplification bandwidth and less transverse spatial walk-off between the interacting beams.

2) Super-Octave, CEP-Stable Seed Generation: Super-octave pulses for seeding OPCPA-based field synthesizers should fulfill four criteria: i) well-behaved and compressible spectral phase, ii) CEP-stability, iii) temporal synchronization with pump pulses, iv) preferably at high pulse energies as the optimum energy ratio between seed and pump pulses results in a higher efficiency and lower amount of superfluorescence [85].

Traditionally, broadband, low-energy oscillators, like Ti:Sapphire were used to seed OPCPAs [86]. Here, the seed pulses have a good temporal contrast, well-behaved spectral phase, and their carrier to envelope phase offset can be actively stabilized [87]. In this scheme, pump and seed pulses

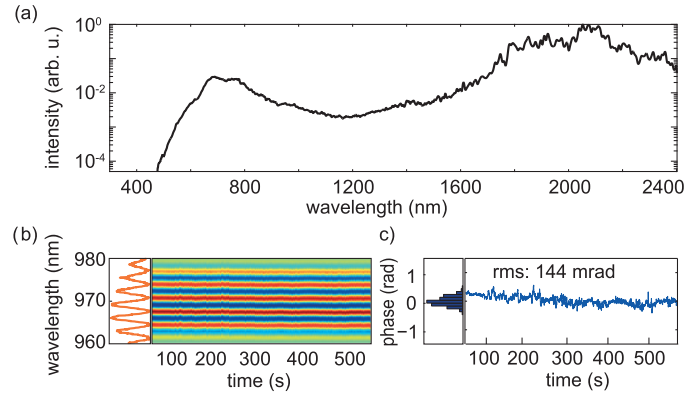

Fig. 5. a) CEP-stable super-octave spectrum generated from a 1-ps Yb:YAG thin-disk regenerative amplifier via several nonlinear processes. b) The resolved fringes in the f-2f interferometer (left) and variation of the f-2f interference pattern over 600 s (right). c) Histogram (left) and reconstructed CEP fluctuations obtained from the f-2f measurement. The retrieved fluctuations yield a 144 mrad CEP jitter over 600 s measurement time (detector's integration time: 4 ms) [84].

are intrinsically synchronized by using one oscillator in the frontend [88]. Slower drifts due to the long optical path of seed and pump pulses, mechanical vibrations of optical components and temperature drifts are compensated by an active temporal synchronization system [89]–[91].

Alternatively, CEP-stable, broadband pulses can be generated directly from the Yb:YAG amplifier by difference-frequency generation (DFG) as an inherently phase-stable process in combination with supercontinuum generation. However, the critical peak power for 1-ps-driven supercontinuum and material damage threshold are of the same order of magnitude, making the generation of a stable spectrum challenging [94]. In an experiment shown by Fattahi *et al.* [84], the 1-ps pulses of a Yb:YAG, thin-disk amplifier were first shortened to 650 fs by using a cross-polarized wave generation [95]. The shortened pulses were later used for supercontinuum generation. As shown by Indra *et al.* [96], alternatively, a 13 cm-long medium can be used to combine the two above-mentioned stages. Afterwards a narrow spectral region of the continuum around 680 nm was amplified in an OPCPA stage to boost the pulse energy and to filter intensity fluctuations. Mixing these amplified pulses with 1030 nm in a Barium borate (BaB_2O_4, BBO) crystal for DFG resulted in CEP-stable pulses ranging from 1700 nm to 2500 nm. Finally the spectral range is extended to visible by supercontinuum generation in a 6 mm YAG crystal as shown in Fig. 5. The efficiency of the scheme can be enhanced by increasing the DFG output energy [97]–[99] and replacing the last supercontinuum generation in bulk by spectral broadening in large mode area fibers [100].

3) Field Synthesis of Optical Parametric Amplifiers: The described super-octave pulses can seed few-fs OPCPA channels pumped by Yb:YAG laser and its harmonics [19], [20]. The CEP-stable supercontinuum can be divided into three spectral regions of comparable bandwidth in the VIS, NIR, and MIR and amplified in the respective OPCPA channels [20], [93] pumped by a 200 mJ Yb:YAG thin-disk regenerative amplifier [49] (see Fig. 6). The amplified pulses of all channels are individually

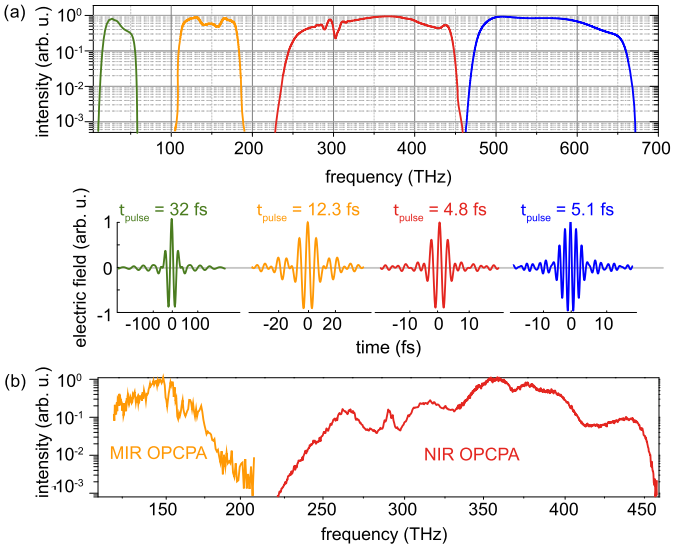

Fig. 6. a) Amplified spectra (top) and the corresponding waveforms (bottom) of the synthesizer's three channels obtained from the simulation with: blue for the visible (VIS) channel, red for near-infrared (NIR), orange for MIR. Extension of the synthesizer's bandwidth to far-infrared can be done by intrapulse difference frequency generation of the MIR channel (the spectrum and the waveform are shown in green). All individual channels support few-cycle pulses [83]. b) The first experimental demonstration of the amplified spectra of the NIR and MIR channels of the waveform synthesizer. In the NIR channel, amplification was done in a 4 mm LBO crystal, pumped by 1 mJ at 515 nm. In the MIR channel, 1 mJ at 1030 nm was used to pump a 2 mm-thick periodically poled $LiNbO_3$ (PPLN) crystal [92], [93].

compressed and combined by a dichroic beam combiner [103] to synthesize sub-cycle to few-cycle NIR to VIS waveforms.

In coherent synthesis of few-cycle pulses, fine control over the spectral phase, the relative phase of each pulse, and their relative timing jitter are crucial. For this purpose, the amplified pulses at each OPCPA channel are sent to delay stages to control the relative phase of each arm. Changing the relative amplitude and relative timing of the three pulses can result in a great variety of sub-cycle optical light transients as shown in Fig. 7.

To ensure a stable light transient at the synthesis point, temporal drifts and relative timing fluctuations between the arms of the synthesizer should be suppressed and compensated to a fraction of the half-field cycle. Using the same source to seed and pump different OPCPA stages reduces the temporal jitter fluctuations to only long term drifts. This remarkable intrinsic temporal synchronization allowed for sampling the electric field of the MIR OPCPA shown in Fig. 6 b) with sub-cycle accuracy and without any active stabilization (Fig. 8) [104]. The MIR pulses were sampled in an electro-optic sampling (EOS) setup [102], containing a 50 μm-thick BBO (Type II) crystal. The 4.8 fs pulses of the NIR OPCPA centered at 1 μm is used as a probe in the EOS setup. Long-term drifts can be compensated by accurate stabilization techniques [18], [105].

4) High Harmonic Generation: mJ-level field synthesizers hold promise to extend the cutoff energy in high harmonic generation (HHG) to kiloelectronvolt (keV) regime at higher photon flux [106]. The HHG cutoff scales with the wavelength, and the peak intensity of the driving pulses. However, the photon flux decreases drastically when longer wavelength sources are used, due to the quantum diffusion. On the other hand, driving pulses with more than two half-cycles and at high peak intensities cause undesirable pre-ionization in the interaction medium and result in depletion of their ground state [107], [108]. The cutoff energy in HHG also depends on the spectral intensity distribution of the waveform. While low-frequency photons tend to extend the cutoff energy, high-frequency photons are desired for the ionization process despite tending to reduce the cutoff energy.

Theoretical study of Wendle *et al.* [109] on the described synthesizer in [20] has shown an optimized, non-sinusoidal light transient can be generated by temporal field synthesis of a few-cycle pulse at 2 μm with weaker few-cycle pulses at second and third harmonic of its carrier frequency. In this study the two accessible experimental parameters: i) relative temporal delay between the three channels of the OPCPA and ii) their relative energy, are scanned and optimized for the highest cutoff energy, highest photon flux, and reduced ionization probability (Fig. 9).

The optimized waveform extends the cutoff energy of isolated attosecond pulses to higher photon flux, compared to few-cycle, 2 μm drivers. This is due to fine tuning of the electron trajectories by using the tailored broadband waveform which leads to the enhancement of the high harmonic yield and extension of the cutoff beyond what is achievable from the synthesis of semi-monochromatic fields at discrete frequencies [110]–[112]. In addition, the lower carrier frequency of such an optimized waveform in comparison to [108], allows for a longer propagation length in the macroscopic scale due to the lower dispersion of longer wavelengths, holds promise to open new frontiers in attosecond physics.

The three-channel few-cycle OPCPA prototype system described above offers a conceptual route for scaling waveform synthesis to the multi-terawatt regime. However, the large footprint of such a concept makes the control of the temporal jitter with sub-cycle resolution cumbersome. To overcome these limitations we propose a new scheme, which obviates the need for active synchronization and reduces the complexity and cost of the systems.

In this scheme which we dub "cross-polarized field synthesis", the optical parametric amplification takes place prior the coherent synthesis. To increase the common beam path of all the OPCPA channels, the super-octave seed pulses are send to an amplification module containing the nonlinear media for the entire broadband seed. Here the separation between different OPCPA channels are not done by their decomposition to several spectral region but with their different polarization state and the proper orientation of different OPCPA crystals. After amplification, the super-octave, high-energy pulses are sent to a field synthesizer similar to [14] for temporal compression and generation of the mJ-light transients at kHz repetition rates. This proposal is discussed in detail in the following section.

C. Cross-Polarized Field Synthesis

Fig. 10 illustrates the OPCPA chain for cross-polarized field synthesis. Super-octave, low-energy, seed pulses with low- and high-frequency parts in orthogonal polarizations are amplified

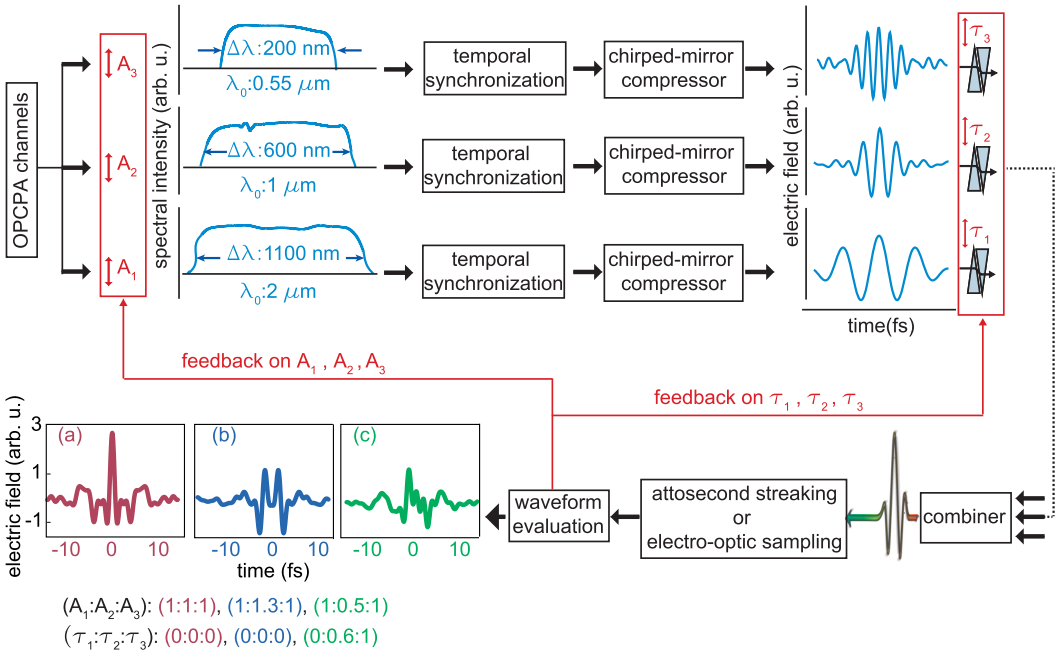

Fig. 7. Detailed setup of the temporal synthesis of the VIS, NIR and MIR pulses. The amplified spectra of all three OPCPA channels centered at 0.55 μm, 1 μm, and 2 μm are first sent through a delay line to achieve a temporal overlap between the synthesizer's three arms. Thereafter the temporally synchronized pulses are compressed to their Fourier transform limit in each arm separately using a set of broadband dielectric chirped mirrors. After passing through a pair of glass wedges to fine tune the relative delay between each arm the three compressed pulses are spatially combined in two broadband dielectric beam combiners. The generated light transients are evaluated using attosecond streaking [101] or electro-optic sampling [102]. By adjusting the relative spectral amplitude of each arm (A_1, A_2, A_3) and their relative phase (τ_1, τ_2, τ_3), a variety of transients can be generated. As an example, panels a), b) and c) show three differently synthesized transients [93].

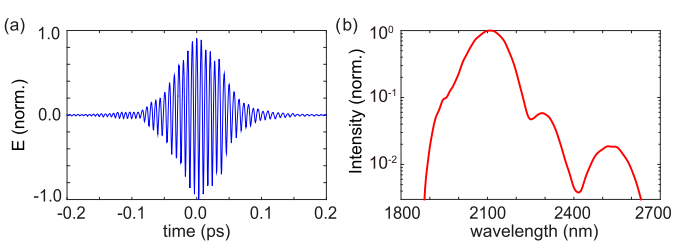

Fig. 8. a) Measured electric filed of the uncompressed MIR pulses in electro-optic sampling and b) its retrieved spectrum.

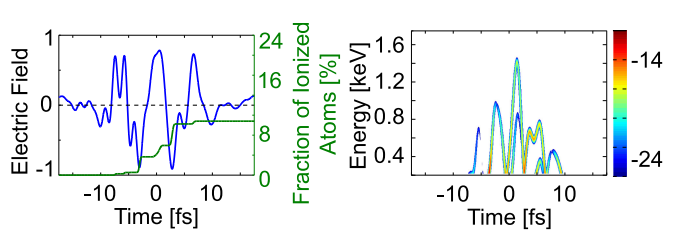

Fig. 9. Electric field, ionization rate (left) and the spectrogram (right) of an optimized waveform with $0.1:0.1:1$ relative energy and $-6:3.6:-0.3$ (fs) delay ratio between the visible, near-infrared, and mid-infrared pulses (VIS:NIR:MIR). The optimized waveform has the cutoff energy of 1.4 keV. The logarithmic color scale represents the harmonic yield [109].

in a hybrid amplification module. The amplifier consists of different nonlinear media suitable for each frequency range and pumped by two high-energy, cross-polarized pump pulses at different frequencies. To maintain an efficient energy transfer

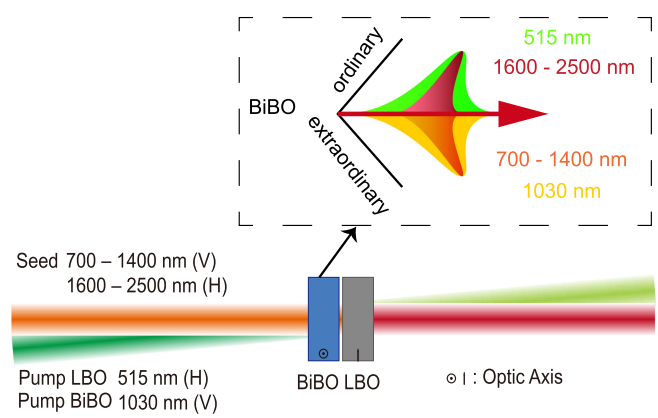

Fig. 10. The concept of cross-polarized OPCPA. The cross-polarized pump beam contains the fundamental beam at 1030 nm, and the second harmonic beam at 515 nm with polarization in vertical (V) and horizontal (H) direction, respectively. The cross-polarized seed beam contains two states of polarizations: vertical direction (V) for 700–1400 nm region and horizontal direction (H) for 1600–2500 nm region. The low-frequency part of the seed spectrum is amplified in the BiBO and the high-frequency part in the LBO crystal. Inset shows how different pump and seed components lie in different axes in the BiBO crystal.

from pump pulses to the broadband seed pulses, the amplification module should be placed within the Rayleigh length of the interacting beams. A noncollinear angle is required for phase-matching and to separate amplified signal from the two pump beams.

Such broadband seed pulses with two states of polarization can be generated by filamentation assisted with

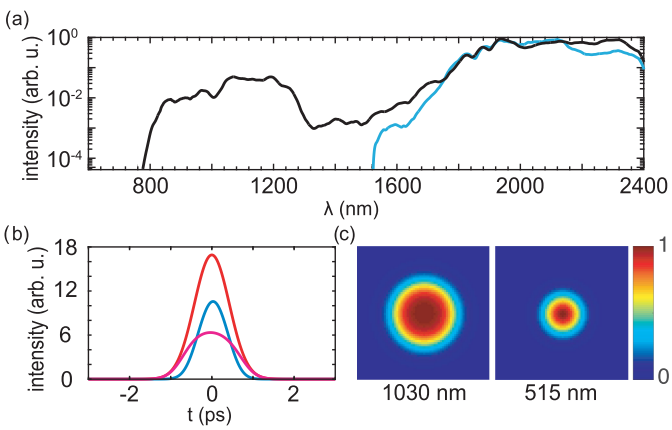

Fig. 11. a) Spectral intensity of the fundamental (blue curve) and the generated cross-polarized supercontinuum (black curve) in a 2 mm thick $LiNbO_3$ crystal. The fundamental part is in the ordinary polarization, and the newly generated 750-1350 nm part lies in the extraordinary polarization, the sum of spectra in both polarizations is shown in black curve [113]. b) The simulated temporal profile of: i) the input pulse before the second harmonic module at 1030 nm with the pulse duration of τ_{FWHM}=1 ps (red curve), ii) the residual of the input pulse after the second harmonic generation at 1030 nm and τ_{FWHM}=1.4 ps (magenta curve), and iii) the generated second harmonic pulse at 515 nm and τ_{FWHM}=0.83 ps. c) The simulated spatial profile of the residual of the input beam after the second harmonic generation at 1030 nm (left) and the generated second harmonic beam at 515 nm (right).

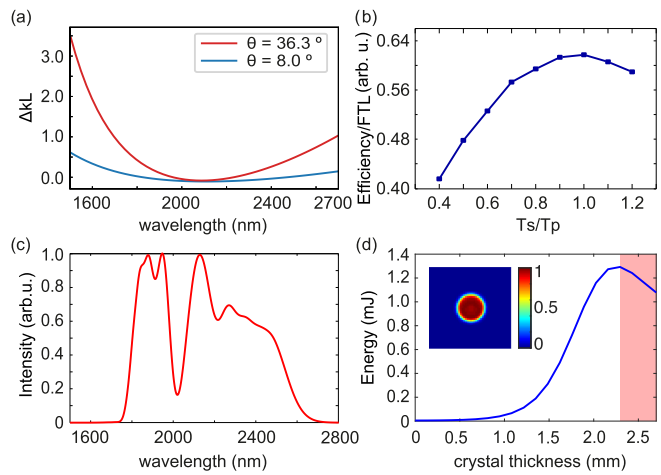

Fig. 12. a) Phase mismatch after 3 mm BiBO in type-I interaction at $\theta = 8.0°$ (blue) and $\theta = 36.3°$ (red) pumped by 1030 nm. b) The ratio of simulated efficiency to Fourier transform limit versus seed-to-pump pulse duration ratio in a 2.4 mm BiBO crystal, assuming a Gaussian temporal profile for pump pulses. c) Simulated amplified spectrum in a 2.3 mm BiBO crystal at $\theta = 8.0°$. d) Simulated amplified pulse energy over crystal length in a 2.7 mm BiBO crystal. The spatiotemporal quality of the amplified pulse degrades in the red shaded region, due to the optical saturation and energy back conversion. Therefore, we choose to stop the amplification at 2.3 mm crystal thickness. The spatial profile of the amplified beam at this thickness is shown in the inset.

cascaded-processes [Fig. 11a] [113]. Here the spectral components from 750 nm to 1400 nm have a crossed polarization relative to the rest of the spectral components.

In what follows we demonstrate the feasibility of amplification of these seed pulses, pumped by an Yb:YAG thin-disk laser described in [55] with a cross-polarized amplification module numerically. For numerical simulations we used SISYFOS which uses Fourier-space method to simulate second-order nonlinear interactions. In this method, each beam is decomposed into plane-wave eigenmodes and the coupled differential equations are solved for the slowly varying eigenmode amplitudes [114].

2 mJ of the output energy of the laser [55] used for generating broadband, CEP stable seed pulses and the rest for pumping the two OPCPA channels. The pump pulses for the NIR region of the spectrum are generated in a frequency converter module comprising a 0.5 mm-thick Type I, BBO crystal. The generated second harmonic with 50% conversion efficiency, has a cross-polarization relative to the fundamental beam. It is smaller in space by a factor of $\sqrt{2}$, due to the second order nonlinearity [see Fig. 11 b) and c)]. After second harmonic generation and prior to the amplification module, the two collinearly propagating beams are separated and recombined. This small module enables a full control for adjusting the pump intensities, and temporal overlaps of the interacting beams in the amplification stage.

1) Mid-Infrared Amplification Module: Bismuth triborate (BiB_3O_6, BiBO) is used as the amplification crystal for the MIR portion of the spectrum, pumped by 1030 nm. Unlike $LiNbO_3$, BiBO is a robust crystal with no photo-refraction and compared to BBO, it supports a broader amplification bandwidth. BiBO is a biaxial crystal. Phase matching condition for the broadband amplification of seed pulses centered at 2 μm is fulfilled for: i) type I, x-z principal plane, $\phi = 0°$, $\theta = 8.0°$ or ii) type I, x-z principal plane, $\phi = 0^{\circ}$, $\theta = 36.3^{\circ}$, at the noncollinear internal seed-pump angle of 1.05°.

TABLE II
SOME OTHER POSSIBLE NONLINEAR PROCESSES IN PARALLEL TO THE PARAMETRIC AMPLIFICATION IN BIBO CLOSE TO $\theta = 8.0°$. PARAMETERS IN BOLD SHOW THE SPECTRAL COMPONENTS OF THE INPUT PULSE

θ (degree)	Interaction	Type	wavelength (nm)
10.6	DFG	I (oo-e)	**2500.0 (o)** + *972.2* (o) = **700.0 (e)**
9.8	DFG	I (oo-e)	**1600.0 (o)** + *1244.4* (o) = **700.0 (e)**
8.5	SFG	I (oo-e)	**2500.0 (o)** + **1600.0 (o)** = *975.6* (e)

The calculated phase mismatch versus the seed frequency for two type-I interactions in BiBO is shown in Fig. 12a). It is clear that at $\theta = 8.0°$ the relative phase mismatch over a broader spectral range is smaller compared to $\theta = 36.3°$. Therefore, we chose type I, BiBO crystal with the phase matching angle of $\theta = 8.0°$.

The polarization of the input interacting beams in type I BiBO crystal is illustrated in Fig. 10. The pump pulses at 1030 nm and the 700 nm to 1400 nm region of the seed spectrum have extraordinary polarization. The 515 nm pump pulses and the 1600 nm to 2500 nm region of the seed spectrum have ordinary polarization. We considered other nonlinear processes which takes place between the four propagating beams and in addition to the parametric amplification of broadband seed pulses at 2 μm. These competitive processes are summarized in Table II. As the efficiency of these processes is very low, they can be neglected.

In an OPCPA, the relative temporal duration of pump and seed pulses and their relative timing play an important role in the amplification process. As it was discussed in Section II-B,

TABLE III
INPUT PARAMETERS FOR SIMULATING THE MIR AMPLIFICATION STAGE. L_c : CRYSTAL LENGTH, D_{eff} : EFFECTIVE NONLINEARITY, α : NONCOLLINEAR INTERNAL SEED-PUMP ANGLE, E_p : PUMP PULSE ENERGY, E_s : SEED PULSE ENERGY, ϕ_p : PUMP BEAM DIAMETER (FWHM), ϕ_s : SEED BEAM DIAMETER (FWHM)

Crystal	L_c (mm)	θ (degree)	ϕ (degree)	d_{eff} (pm/V)
BiBO	2.3	8	0	2.04
α (degree)	E_p (mJ)	E_s (mJ)	ϕ_p (mm)	ϕ_s (mm)
1.05	9	0.005	2.29	2.4

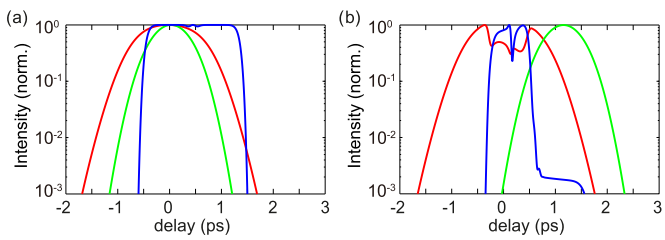

Fig. 13. a) The normalized temporal profile of the unamplified seed at 700-2500 nm (blue), and input 1030 nm (red) and 515 nm (green) pump pulses used for the simulation. b) The simulated normalized temporal profile of the amplified seed at 700-2500 nm (blue), and the 1030 nm (red) and 515 nm (green) pump pulses after the BiBO crystal. The 1750 nm to 2500 nm part of the seed is amplified, and the 515 nm pump is delayed and overlapped with the latter half of the seed.

the optimum pump pulse duration to reach a broad amplification bandwidth as well as a high conversion efficiency lies in the range of 1-10 ps. We studied the optimum relative seed-to-pump pulse durations, in a series of simulations by varying the seed pulse duration from 400 fs to 1.2 ps in the MIR amplification module. The optical efficiency to Fourier transform limit ratio of the amplified spectrum is defined as a figure of merit for different relative seed-to-pump temporal durations. As shown in Fig. 12b), seed-to-pump duration ratio of 1.0 appears as the optimum value. Assuming a flat-top spatio-temporal profile for the pump pulses at 1030 nm shifts this ratio to 1.1. However, in the following simulations we chose seed-to-pump duration ratio of 0.65 for the MIR channel and 1.1 for the NIR channel as they support a slightly broader amplification bandwidth and ease the demands on the broadband seed stretcher prior to the amplification.

Fig. 12c) shows the spectrum of the 1.3 mJ amplified MIR region in a 2.3-mm-thick BiBO, corresponding to an optical-to-optical conversion efficiency of 14.5%. The amplification was stopped before the back-conversion of energy from the idler and signal to the pump overtakes the process and degrade the spatio-temporal profile of the signal (Fig. 12d)). Input parameters of the numerical simulation are summarized in Table III. The beam size of 1030 nm pump is adjusted to reach the peak intensity of 100 GW/cm^2 at the crystal.

After the first amplification crystal, the pump pulses centered at 515 nm are delayed relative to their counterpart at 1030 nm by 1.15 ps and are temporally overlapped with the NIR region of the input seed pulses (see Fig. 13).

2) Near-Infrared Amplification Module: In the NIR portion of the spectrum, a broadband amplification gain can be obtained in Lithiu m triborate (LiB_3O_5, LBO) crystal at the noncollinear internal seed-pump angle of 1.05°, and a phase-matching angle of $\phi = 15°$. As this phase-matching angle also supports the frequency doubling of the 1030 nm pump pulses, we chose to place LBO after the BiBO crystal.

TABLE IV
INPUT PARAMETERS FOR SIMULATING THE NIR AMPLIFICATION STAGE. L_c : CRYSTAL LENGTH, D_{eff} : EFFECTIVE NONLINEARITY, α : NONCOLLINEAR INTERNAL SEED-PUMP ANGLE, E_p : PUMP PULSE ENERGY, E_s : SEED PULSE ENERGY, ϕ_p : PUMP BEAM DIAMETER (FWHM), ϕ_s : SEED BEAM DIAMETER (FWHM)

Crystal	L_c (mm)	θ (degree)	ϕ (degree)	d_{eff} (pm/V)
LBO	3	90	15	0.819
α (degree)	E_p (mJ)	E_s (mJ)	ϕ_p (mm)	ϕ_s (mm)
1.05	9	0.005	3.05	2.4

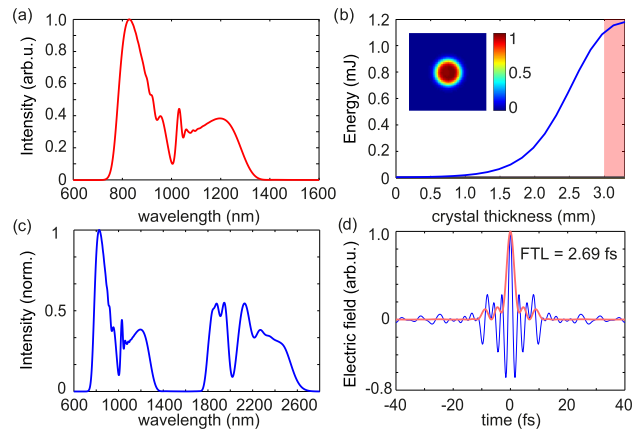

Fig. 14. a) Simulated amplified spectrum in a 3 mm LBO crystal. b) Simulated amplified pulse energy over crystal length in a 3.3 mm LBO crystal. The spatiotemporal quality of the amplified pulse degrades in the red shaded region, due to the optical saturation and energy back conversion. Therefore, we choose to stop the amplification at 3.0 mm. The spatial profile of the amplified beam at this thickness is shown in the inset. c) Simulated amplified spectra in BiBO and LBO crystals. The shown spectra are normalized to the relative amplified energy of both stages. d) The calculated temporal electric field (blue) of the spectrum shown in (c), and it's temporal intensity (red). The Fourier transform limit of the amplified spectrum shown in (c) is 2.69 fs.

The input parameters for numerical simulation of the NIR amplification stage are summarized in Table IV. The beam size of 515 nm pump is adjusted to reach the peak intensity of 100 GW/cm^2 at the crystal.

Fig. 14 shows the spectrum, and the amplified energy versus crystal length for the 1.1 mJ amplified signal pulses in a 3 mm-thick LBO crystal with the optical conversion efficiency of 12.3%. The only significant parasitic process in the NIR amplification module is the second harmonic generation of the amplified seed pulses, as the NIR spectral region becomes temporally separated from the 1030 nm pump pulses (see Fig. 13 b)). This effect is considered in the simulation.

Afterwards amplification the seed pulses are separated by their polarization state, each arm is compressed to its Fourier limit and finally recombined by a dichroic mirror. Fig. 14 d) shows the calculated, mJ-level light transient, that is generated in such a scheme.

III. CONCLUSION

Advancing the frontiers of high peak- and average-power tailored light transients can open up unprecedented opportunities in

attosecond and high-field physics. In this review we presented a road-map towards this exciting horizon based on Yb-YAG thin-disk laser technology. We have discussed three alternative approaches to this end: i) direct and efficient spectral broadening of high-energy and high-power Yb:YAG lasers, ii) coherent combination and synthesis of pulses from multiple parallel broadband OPAs, and iii) coherent combination and synthesis of a superoctave serial OPAs. For the first two options, we also presented the experimental results, the current status, and the missing building blocks for their realization.

We presented up to 11-fold efficient spectral broadening of Yb:YAG, high-energy regenerative amplifiers and high-power oscillators in a phase-induced multi-pass broadening scheme. Shorter pulses are generated in a consecutive cells or by combining this approach with fiber-based supercontinuum generation [64]. If the CEP-stability of these laser sources is realized, their combination with field synthesis enables the generation of high-energy and high-power light transients in a smaller footprint and a more robust system.

Afterwords, a full conceptual study on field synthesis of three parallel OPCPAs was presented. Different approaches to generate a CEP-stable super-octave seed spectrum for the multi channel OPCPAs and directly from the Yb:YAG lasers were studied. This crucial step allows for intrinsic synchronization between the pump and seed pulses at the OPCPA stages and relaxes the demands on active temporal stabilization. We presented the preliminary results on the amplification of the two channels of the designed system. We also showed the first direct sampling of the electric field of the MIR OPCPA by using its counterpart NIR OPCPA channel. It was also shown numerically that the optimized light transient from such a synthesizer results in extending the cutoff energy in HHG with higher photon flux.

Finally, we numerically studied the design of a mJ-level serial multi-channel OPCPA chain. Here, different spectral regions are not separated physically. Rather different OPCPA channels are distinguished by their state of polarization. The common beam path in this design, enhances the stability, reduces the footprint and complexity, and decreases the temporal jitter initiated from systematic complexity.

Ultrashort pulses has been a versatile tool for controlling strong-field interactions at several femtosecond time scale. Tailored light transients at petahertz frequencies are about to change the state-of-the art, by enabling the sub-cycle control of fast phenomena.

References

[1] A. Y. Piggott *et al.*, "Inverse design and demonstration of a compact and broadband on-chip wavelength demultiplexer," *Nature Photon.*, vol. 9, no. 6, pp. 374–377, Jun. 2015. [Online]. Available: http://www.nature.com/articles/nphoton.2015.69

[2] J. Lu and J. Vučković, "Nanophotonic computational design," *Opt. Exp.*, vol. 21, no. 11, pp. 13351–13367, Jun. 2013. [Online]. Available: https://www.osapublishing.org/oe/abstract.cfm?uri=oe-21-11-13351

[3] F. Krausz and M. I. Stockman, "Attosecond metrology: From electron capture to future signal processing," *Nature Photon.*, vol. 8, no. 3, pp. 205–213, Mar. 2014. [Online]. Available: http://www.nature.com/articles/nphoton.2014.28 http://www.nature.com/articles/nphoton.2014.28

[4] G. Vampa, H. Fattahi, J. Vučković, and F. Krausz, "Nonlinear optics: Attosecond nanophotonics," *Nature Photon.*, vol. 11, no. 4, pp. 210–212, Apr. 2017. [Online]. Available: http://www.nature.com/doifinder/10.1038/nphoton.2017.41

[5] A. Sommer *et al.*, "Attosecond nonlinear polarization and lightmatter energy transfer in solids," *Nature*, vol. 534, no. 7605, pp. 86–90, May 2016. [Online]. Available: http://www.nature.com/doifinder/10.1038/nature17650

[6] A. M. Weiner, D. E. Leaird, G. P. Wiederrecht, and K. A. Nelson, "Femtosecond pulse sequences used for optical manipulation of molecular motion," *Science*, vol. 247, no. 4948, pp. 1317–1319, Mar. 1990. [Online]. Available: http://www.ncbi.nlm.nih.gov/pubmed/17843793 http://www.sciencemag.org/cgi/doi/10.1126/science.247.4948.1317

[7] O. E. Martinez, J. P. Gordon, and R. L. Fork, "Negative group-velocity dispersion using refraction," *J. Opt. Soc. Amer. A*, vol. 1, no. 10, pp. 1003–1006, Oct. 1984. [Online]. Available: https://www.osapublishing.org/abstract.cfm?URI=josaa-1-10-1003

[8] E. Treacy, "Optical pulse compression with diffraction gratings," *IEEE J. Quantum Electron.*, vol. QE-5, no. 9, pp. 454–458, Sep. 1969. [Online]. Available: http://ieeexplore.ieee.org/document/1076303/

[9] O. Razskazovskaya, F. Krausz, and V. Pervak, "Multilayer coatings for femto- and attosecond technology," *Optica*, vol. 4, no. 1, p. 129, Jan. 2017. [Online]. Available: https://www.osapublishing.org/abstract.cfm?URI=optica-4-1-129

[10] A. Weiner, D. Leaird, J. Patel, and J. Wullert, "Programmable shaping of femtosecond optical pulses by use of 128-element liquid crystal phase modulator," *IEEE J. Quantum Electron.*, vol. 28, no. 4, pp. 908–920, Apr. 1992. [Online]. Available: http://ieeexplore.ieee.org/document/135209/

[11] S. T. Cundiff and A. M. Weiner, "Optical arbitrary waveform generation," *Nature Photon.*, vol. 4, no. 11, pp. 760–766, Nov. 2010. [Online]. Available: http://www.nature.com/articles/nphoton.2010.196

[12] F. Verluise, V. Laude, Z. Cheng, C. Spielmann, and P. Tournois, "Amplitude and phase control of ultrashort pulses by use of an acousto-optic programmable dispersive filter: pulse compression and shaping," *Opt. Lett.*, vol. 25, no. 8, pp. 575–577, Apr. 2000. [Online]. Available: https://www.osapublishing.org/abstract.cfm?URI=ol-25-8-575

[13] A. Wirth *et al.*, "Synthesized light transients," *Science*, vol. 334, no. 6053, pp. 195–200, Oct. 2011. [Online]. Available: http://www.sciencemag.org/content/334/6053/195

[14] M. T. Hassan *et al.*, "Invited article: Attosecond photonics: synthesis and control of light transients," *Rev. Sci. Instrum.*, vol. 83, no. 11, pp. 1113011–1113019, Nov. 2012. [Online]. Available: http://www.ncbi.nlm.nih.gov/pubmed/23206044

[15] G. Cerullo, A. Baltuška, O. Mücke, and C. Vozzi, "Few-optical-cycle light pulses with passive carrier-envelope phase stabilization," *Laser Photon. Rev.*, vol. 5, no. 3, pp. 323–351, May 2011. [Online]. Available: http://doi.wiley.com/10.1002/lpor.201000013

[16] T. T. Luu *et al.*, "Extreme ultraviolet high-harmonic spectroscopy of solids," *Nature*, vol. 521, no. 7553, pp. 498–502, May 2015. [Online]. Available: http://www.nature.com/doifinder/10.1038/nature14456

[17] M. T. Hassan *et al.*, "Optical attosecond pulses and tracking the nonlinear response of bound electrons," *Nature*, vol. 530, no. 7588, pp. 66–70, Feb. 2016. [Online]. Available: http://www.nature.com/doifinder/10.1038/nature16528

[18] C. Manzoni *et al.*, "Coherent synthesis of ultra-broadband optical parametric amplifiers," *Opt. Lett.*, vol. 37, no. 11, pp. 1880–1882, Jun. 2012. [Online]. Available: http://www.ncbi.nlm.nih.gov/pubmed/22660060

[19] O. D. Mucke *et al.*, "Toward waveform nonlinear optics using multimillijoule sub-cycle waveform synthesizers," *IEEE J. Sel. Topics Quantum Electron.*, vol. 21, no. 5, Sep. 2015, Art. no. 8700712. [Online]. Available: https://ieeexplore.ieee.org/document/7095515

[20] H. Fattahi *et al.*, "Third-generation femtosecond technology," *Optica*, vol. 1, no. 1, pp. 45–63, Jul. 2014. [Online]. Available: http://www.opticsinfobase.org/optica/abstract.cfm?URI=optica-1-1-45

[21] C. Manzoni *et al.*, "Coherent pulse synthesis: Towards sub-cycle optical waveforms," *Laser Photon. Rev.*, vol. 9, no. 2, pp. 129–171, Mar. 2015. [Online]. Available: http://doi.wiley.com/10.1002/lpor.201400181

[22] M. Schulz *et al.*, "Yb:YAG Innoslab amplifier: Efficient high repetition rate subpicosecond pumping system for optical parametric chirped pulse amplification," *Opt. Lett.*, vol. 36, no. 13, pp. 2456–2458, Jul. 2011. [Online]. Available: http://ol.osa.org/abstract.cfm?URI=ol-36-13-2456

[23] B. E. Schmidt, A. Hage, T. Mans, F. Légaré, and H. J. Wörner, "Highly stable, 54mJ Yb-InnoSlab laser platform at 05 kW average power," *Opt. Express*, vol. 25, no. 15, pp. 17549–17555, Jul. 2017. [Online]. Available: https://www.osapublishing.org/abstract.cfm?URI=oe-25-15-17549

[24] P. Russbueldt, T. Mans, J. Weitenberg, H. D. Hoffmann, and R. Poprawe, "Compact diode-pumped 11 kW Yb:YAG Innoslab femtosecond amplifier," *Opt. Lett.*, vol. 35, no. 24, pp. 4169–4171, Dec. 2010. [Online]. Available: https://www.osapublishing.org/abstract.cfm?URI=ol-35-24-4169

[25] P. Russbueldt *et al.*, "400 W Yb:YAG Innoslab fs-Amplifier," *Opt. Express*, vol. 17, no. 15, pp. 12230–12245, Jul. 2009. [Online]. Available: https://www.osapublishing.org/oe/abstract.cfm?uri=oe-17-15-12230

[26] M. Puppin *et al.*, "500 kHz OPCPA delivering tunable sub-20 fs pulses with 15 W average power based on an all-ytterbium laser," *Opt. Express*, vol. 23, no. 2, pp. 1491–1497, Jan. 2015. [Online]. Available: https://www.osapublishing.org/oe/abstract.cfm?uri=oe-23-2-1491

[27] V. Markovic *et al.*, "160 W 800 fs Yb:YAG single crystal fiber amplifier without CPA," *Opt. Express*, vol. 23, no. 20, pp. 25883–25888, Oct. 2015. [Online]. Available: https://www.osapublishing.org/abstract.cfm?URI=oe-23-20-25883

[28] X. Délen *et al.*, "Yb:YAG single crystal fiber power amplifier for femtosecond sources," *Opt. Lett.*, vol. 38, no. 2, pp. 109–111, Jan. 2013. [Online]. Available: https://www.osapublishing.org/abstract.cfm?URI=ol-38-2-109

[29] F. Lesparre *et al.*, "Yb:YAG single-crystal fiber amplifiers for picosecond lasers using the divided pulse amplification technique," *Opt. Lett.*, vol. 41, no. 7, pp. 1628–1631, Apr. 2016. [Online]. Available: https://www.osapublishing.org/abstract.cfm?URI=ol-41-7-1628

[30] J. Rothhardt *et al.*, "100 W average power femtosecond laser at 343 nm," *Opt. Lett.*, vol. 41, no. 8, pp. 1885–1888, Apr. 2016. [Online]. Available: https://www.osapublishing.org/abstract.cfm?URI=ol-41-8-1885

[31] S. Tokita, J. Kawanaka, Y. Izawa, M. Fujita, and T. Kawashima, "23.7-W picosecond cryogenic-Yb:YAG multipass amplifier," *Opt. Exp.*, vol. 15, no. 7, pp. 3955–3961, 2007. [Online]. Available: https://www.osapublishing.org/oe/abstract.cfm?uri=oe-15-7-3955

[32] K.-H. Hong *et al.*, "Generation of 287 W, 55 ps pulses at 78 MHz repetition rate from a cryogenically cooled Yb:YAG amplifier seeded by a fiber chirped-pulse amplification system," *Opt. Lett.*, vol. 33, no. 21, pp. 2473–2475, Nov. 2008. [Online]. Available: https://www.osapublishing.org/abstract.cfm?URI=ol-33-21-2473

[33] K.-H. Hong *et al.*, "High-energy, kHz-repetition-rate, ps cryogenic Yb:YAG chirped-pulse amplifier," *Opt. Lett.*, vol. 35, no. 11, pp. 1752–1754, Jun. 2010. [Online]. Available: https://www.osapublishing.org/abstract.cfm?URI=ol-35-11-1752

[34] L. E. Zapata, F. Reichert, M. Hemmer, and F. X. Kärtner, "250 W average power, 100 kHz repetition rate cryogenic Yb:YAG amplifier for OPCPA pumping," *Opt. Lett.*, vol. 41, no. 3, pp. 492–495, Feb. 2016. [Online]. Available: https://www.osapublishing.org/abstract.cfm?URI=ol-41-3-492

[35] D. C. Brown, J. M. Singley, K. Kowalewski, J. Guelzow, and V. Vitali, "High sustained average power cw and ultrafast Yb:YAG near-diffraction-limited cryogenic solid-state laser," *Opt. Exp.*, vol. 18, no. 24, pp. 24770–24792, Nov. 2010. [Online]. Available: https://www.osapublishing.org/oe/abstract.cfm?uri=oe-18-24-24770

[36] B. A. Reagan *et al.*, "1 Joule, 100 Hz repetition rate, picosecond CPA laser for driving high average power soft X-ray lasers," in *Proc. Conf. Lasers Electro-Opt.*, Washington, DC, USA, 2014, Paper SM1F.4. [Online]. Available: https://www.osapublishing.org/abstract.cfm?URI=CLEO_SI-2014-SM1F.4

[37] M. Hemmer *et al.*, "Picosecond, 115 mJ energy, 200 Hz repetition rate cryogenic Yb:YAG bulk-amplifier," in *Proc. Conf. Lasers Electro-Opt.*, Washington, DC, OSA, 2015, Paper STu4O.3. [Online]. Available: https://www.osapublishing.org/abstract.cfm?URI=CLEO_SI-2015-STu4O.3

[38] J. Smith *et al.*, "100J-level nanosecond pulsed Yb:YAG cryo-cooled DPSSL amplifier," in *Solid State Lasers XXVII: Technology and Devices*, W. A. Clarkson and R. K. Shori, Eds. Bellingham, WA, USA: SPIE, Feb. 2018, p. 27. [Online]. Available: https://www.spiedigitallibrary.org/conference-proceedings-of-spie/10511/2289579/100J-level-nanosecond-pulsed-YbYAG-cryo-cooled-DPSSL-amplifier/10.1117/12.2289579.full

[39] C. Baumgarten *et al.*, "1 J, 05 kHz repetition rate picosecond laser," *Opt. Lett.*, vol. 41, no. 14, pp. 3339–3342, Jul. 2016. [Online]. Available: https://www.osapublishing.org/abstract.cfm?URI=ol-41-14-3339

[40] L. E. Zapata *et al.*, "Cryogenic Yb:YAG composite-thin-disk for high energy and average power amplifiers," *Opt. Lett.*, vol. 40, no. 11, pp. 2610–2613, Jun. 2015. [Online]. Available: https://www.osapublishing.org/ol/abstract.cfm?uri=ol-40-11-2610

[41] C.-L. Chang *et al.*, "High-energy, kHz, picosecond hybrid Yb-doped chirped-pulse amplifier," *Opt. Exp.*, vol. 23, no. 8, pp. 10132–10144, Apr. 2015. [Online]. Available: https://www.osapublishing.org/abstract.cfm?URI=oe-23-8-10132

[42] T. Metzger *et al.*, "High-repetition-rate picosecond pump laser based on a Yb:YAG disk amplifier for optical parametric amplification," *Opt. Lett.*, vol. 34, no. 14, pp. 2123–2125, Jul. 2009. [Online]. Available: https://www.osapublishing.org/abstract.cfm?URI=ol-34-14-2123

[43] O. Pronin *et al.*, "High-power 200 fs Kerr-lens mode-locked Yb:YAG thin-disk oscillator," *Opt. Lett.*, vol. 36, no. 24, pp. 4746–4748, Dec. 2011. [Online]. Available: https://www.osapublishing.org/abstract.cfm?URI=ol-36-24-4746

[44] J. Novák *et al.*, "Thin disk amplifier-based 40 mJ, 1 kHz, picosecond laser at 515 nm," *Opt. Exp.*, vol. 24, no. 6, pp. 5728–5733, Mar. 2016. [Online]. Available: https://www.osapublishing.org/abstract.cfm?URI=oe-24-6-5728

[45] F. Batysta *et al.*, "Broadband OPCPA system with 11 mJ output at 1 kHz, compressible to 12 fs," *Opt. Exp.*, vol. 24, no. 16, pp. 17843–17848, Aug. 2016. [Online]. Available: https://www.osapublishing.org/abstract.cfm?URI=oe-24-16-17843

[46] S. Prinz *et al.*, "Thin-disk pumped optical parametric chirped pulse amplifier delivering CEP-stable multi-mJ few-cycle pulses at 6 kHz," *Opt. Express*, vol. 26, no. 2, pp. 1108–1124, Jan. 2018. [Online]. Available: https://www.osapublishing.org/abstract.cfm?URI=oe-26-2-1108

[47] J.-P. Negel *et al.*, "Ultrafast thin-disk multipass laser amplifier delivering 14 kW (47 mJ, 1030 nm) average power converted to 820 W at 515 nm and 234 W at 343 nm," *Opt. Express*, vol. 23, no. 16, Aug. 2015, Art. no. 21064. [Online]. Available: https://www.osapublishing.org/abstract.cfm?URI=oe-23-16-21064

[48] R. Jung, J. Tümmler, and I. Will, "Regenerative thin-disk amplifier for 300 mJ pulse energy," *Opt. Exp.*, vol. 24, no. 2, pp. 883–887, Jan. 2016. [Online]. Available: https://www.osapublishing.org/abstract.cfm?URI=oe-24-2-883

[49] T. Nubbemeyer *et al.*, "1 kW, 200 mJ picosecond thin-disk laser system," *Opt. Lett.*, vol. 42, no. 7, pp. 1381–1384, Apr. 2017. [Online]. Available: https://www.osapublishing.org/abstract.cfm?URI=ol-42-7-1381

[50] D. Bauer, I. Zawischa, D. H. Sutter, A. Killi, and T. Dekorsy, "Mode-locked Yb:YAG thin-disk oscillator with 41 J pulse energy at 145 W average infrared power and high power frequency conversion," *Opt. Express*, vol. 20, no. 9, pp. 9698–9704, Apr. 2012. [Online]. Available: https://www.osapublishing.org/oe/abstract.cfm?uri=oe-20-9-9698

[51] S. V. Marchese *et al.*, "Femtosecond thin disk laser oscillator with pulse energy beyond the 10-microjoule level," *Opt. Express*, vol. 16, no. 9, pp. 6397–6407, Apr. 2008. [Online]. Available: https://www.osapublishing.org/oe/abstract.cfm?uri=oe-16-9-6397

[52] S. V. Marchese, T. Südmeyer, M. Golling, R. Grange, and U. Keller, "Pulse energy scaling to 5 μJ from a femtosecond thin disk laser," *Opt. Lett.*, vol. 31, no. 18, pp. 2728–2730, Sep. 2006. [Online]. Available: https://www.osapublishing.org/abstract.cfm?URI=ol-31-18-2728

[53] F. Beirow *et al.*, "Radially polarized passively mode-locked thin-disk laser oscillator emitting sub-picosecond pulses with an average output power exceeding the 100 W level," *Opt. Exp.*, vol. 26, no. 4, pp. 4401–4410, Feb. 2018. [Online]. Available: https://www.osapublishing.org/abstract.cfm?URI=oe-26-4-4401

[54] W. Schneider *et al.*, "800-fs, 330-μJ pulses from a 100-W regenerative Yb:YAG thin-disk amplifier at 300 kHz and THz generation in LiNbO_3," *Opt. Lett.*, vol. 39, no. 23, pp. 6604–6607, Dec. 2014. [Online]. Available: https://www.osapublishing.org/abstract.cfm?URI=ol-39-23-6604

[55] H. Fattahi *et al.*, "High-power, 1-ps, all-Yb:YAG thin-disk regenerative amplifier," *Opt. Lett.*, vol. 41, no. 6, pp. 1126–1129, Mar. 2016. [Online]. Available: https://www.osapublishing.org/abstract.cfm?URI=ol-41-6-1126

[56] B.-H. Chen *et al.*, "Compression of picosecond pulses from a thin-disk laser to 30 fs at 4 W average power," *Opt. Exp.*, vol. 26, no. 4, pp. 3861–3869, Feb. 2018. [Online]. Available: https://www.osapublishing.org/abstract.cfm?URI=oe-26-4-3861

[57] M. Ueffing *et al.*, "Direct regenerative amplification of femtosecond pulses to the multimillijoule level," *Opt. Lett.*, vol. 41, no. 16, pp. 3840–3843, Aug. 2016. [Online]. Available: https://www.osapublishing.org/abstract.cfm?URI=ol-41-16-3840

[58] J. Koerner *et al.*, "Measurement of temperature-dependent absorption and emission spectra of Yb:YAG, Yb:LuAG, and Yb:CaF_2 between 20 C and 200 C and predictions on their influence on laser performance," *J. Opt. Soc. Amer. B*, vol. 29, no. 9, pp. 2493–2502, Sep. 2012. [Online]. Available: https://www.osapublishing.org/abstract.cfm?URI=josab-29-9-2493

[59] M. Nisoli, S. De Silvestri, and O. Svelto, "Generation of high energy 10 fs pulses by a new pulse compression technique," *Appl. Phys. Lett.*, vol. 68, no. 20, pp. 2793–2795, May 1996. [Online]. Available: http://aip.scitation.org/doi/10.1063/1.116609

[60] S. Hädrich *et al.*, "Energetic sub-2-cycle laser with 216 W average power," *Opt. Lett.*, vol. 41, no. 18, pp. 4332–4335, Sep. 2016. [Online]. Available: https://www.osapublishing.org/abstract.cfm?URI=ol-41-18-4332

[61] J. Schulte, T. Sartorius, J. Weitenberg, A. Vernaleken, and P. Russbueldt, "Nonlinear pulse compression in a multi-pass cell," *Opt. Lett.*, vol. 41, no. 19, pp. 4511–4514, Oct. 2016. [Online]. Available: https://www.osapublishing.org/abstract.cfm?URI=ol-41-19-4511

[62] J. Weitenberg *et al.*, "Multi-pass-cell-based nonlinear pulse compression to 115 fs at 75 J pulse energy and 300 W average power," *Opt. Exp.*, vol. 25, no. 17, pp. 20502–20510, Aug. 2017. [Online]. Available: https://www.osapublishing.org/abstract.cfm?URI=oe-25-17-20502

[63] M. Ueffing *et al.*, "Nonlinear pulse compression in a gas-filled multipass cell," *Opt. Lett.*, vol. 43, no. 9, pp. 2070–2073, May 2018. [Online]. Available: https://www.osapublishing.org/abstract.cfm?URI=ol-43-9-2070

[64] G. Barbiero *et al.*, "Towards 45 watt single-cycle pulses from Yb:YAG thin-disk oscillators," presented at the *Conf. Lasers Electro-Optics (CLEO)*, Munich, Germany, 2019.

[65] K. Fritsch, M. Poetzlberger, V. Pervak, J. Brons, and O. Pronin, "All-solid-state multipass spectral broadening to sub-20 fs," *Opt. Lett.*, vol. 43, no. 19, pp. 4643–4646, Oct. 2018. [Online]. Available: https://www.osapublishing.org/abstract.cfm?URI=ol-43-19-4643

[66] M. Kaumanns *et al.*, "Multipass spectral broadening of 18 mJ pulses compressible from 1.3 ps to 41 fs," *Opt. Lett.*, vol. 43, no. 23, pp. 5877–5880, Dec. 2018. [Online]. Available: https://www.osapublishing.org/abstract.cfm?URI=ol-43-23-5877

[67] F. Emaury *et al.*, "Frequency comb offset dynamics of SESAM mode-locked thin disk lasers," *Opt. Express*, vol. 23, no. 17, pp. 21836–21856, Aug. 2015. [Online]. Available: https://www.osapublishing.org/abstract.cfm?URI=oe-23-17-21836

[68] N. Modsching *et al.*, "Carrier-envelope offset frequency stabilization of a thin-disk laser oscillator operating in the strongly self-phase modulation broadened regime," *Opt. Express*, vol. 26, no. 22, pp. 28461–28468, Oct. 2018. [Online]. Available: https://www.osapublishing.org/abstract.cfm?URI=oe-26-22-28461

[69] O. Pronin *et al.*, "High-power multi-megahertz source of waveform-stabilized few-cycle light," *Nature Commun.*, vol. 6, no. 1, Dec. 2015, Art. no. 6988. [Online]. Available: http://www.nature.com/articles/ncomms7988

[70] M. Seidel *et al.*, "Carrier-envelope-phase stabilization via dual wavelength pumping," *Opt. Lett.*, vol. 41, no. 8, pp. 1853–1856, Apr. 2016. [Online]. Available: https://www.osapublishing.org/abstract.cfm?URI=ol-41-8-1853

[71] J. Rothhardt, S. Demmler, S. Hädrich, J. Limpert, and A. Tünnermann, "Octave-spanning OPCPA system delivering CEP-stable few-cycle pulses and 22 W of average power at 1 MHz repetition rate," *Opt. Express*, vol. 20, no. 10, pp. 10870–10878, May 2012. [Online]. Available: https://www.osapublishing.org/oe/abstract.cfm?uri=oe-20-10-10870

[72] S. Prinz *et al.*, "CEP-stable, sub-6 fs, 300-kHz OPCPA system with more than 15 W of average power," *Opt. Express*, vol. 23, no. 2, pp. 1388–1394, Jan. 2015. [Online]. Available: https://www.osapublishing.org/abstract.cfm?URI=oe-23-2-1388

[73] D. Herrmann *et al.*, "Generation of sub-three-cycle, 16 TW light pulses by using noncollinear optical parametric chirped-pulse amplification," *Opt. Lett.*, vol. 34, no. 16, pp. 2459–5461, Aug. 2009. [Online]. Available: https://www.osapublishing.org/abstract.cfm?URI=ol-34-16-2459

[74] R. Budrinas *et al.*, "53 W average power CEP-stabilized OPCPA system delivering 55 TW few cycle pulses at 1 kHz repetition rate," *Opt. Exp.*, vol. 25, no. 5, pp. 5797–5806, Mar. 2017. [Online]. Available: https://www.osapublishing.org/abstract.cfm?URI=oe-25-5-5797

[75] G. M. Gale, M. Cavallari, T. J. Driscoll, and F. Hache, "Sub-20-fs tunable pulses in the visible from an 82-MHz optical parametric oscillator," *Opt. Lett.*, vol. 20, no. 14, pp. 1562–1564, Jul. 1995. [Online]. Available: http://www.opticsinfobase.org/abstract.cfm?URI=ol-20-14-1562

[76] G. M. Gale, M. Cavallari, and F. Hache, "Femtosecond visible optical parametric oscillator," *J. Opt. Soc. Amer. B*, vol. 15, no. 2, pp. 702–714, Feb. 1998. [Online]. Available: http://www.opticsinfobase.org/abstract.cfm?URI=josab-15-2-702

[77] Y. Deng *et al.*, "Carrier-envelope-phase-stable, 1.2 mJ, 1.5 cycle laser pulses at 2.1 μm," *Opt. Lett.*, vol. 37, no. 23, pp. 4973–4975, Dec. 2012. [Online]. Available: http://ol.osa.org/abstract.cfm?URI=ol-37-23-4973

[78] B. E. Schmidt *et al.*, "Frequency domain optical parametric amplification," *Nature Commun.*, vol. 5, pp. 36431–36438, Jan. 2014. [Online]. Available: http://www.nature.com/ncomms/2014/140507/ncomms4643/full/ncomms4643.html

[79] N. Bigler *et al.*, "High-power OPCPA generating 17 cycle pulses at 25 m," *Opt. Express*, vol. 26, no. 20, pp. 26750–26757, Oct. 2018. [Online]. Available: https://www.osapublishing.org/abstract.cfm?URI=oe-26-20-26750

[80] K.-H. Hong *et al.*, "Multi-mJ, kHz, 21 μm optical parametric chirped-pulse amplifier and high-flux soft x-ray high-harmonic generation," *Opt. Lett.*, vol. 39, no. 11, pp. 3145–3148, Jun. 2014. [Online]. Available: https://www.osapublishing.org/abstract.cfm?URI=ol-39-11-3145

[81] Y. Yin *et al.*, "High-efficiency optical parametric chirped-pulse amplifier in BiB_3O_6 for generation of 3 mJ, two-cycle, carrier-envelope-phase-stable pulses at 17 μm," *Opt. Lett.*, vol. 41, no. 6, pp. 1142–1145, Mar. 2016. [Online]. Available: https://www.osapublishing.org/abstract.cfm?URI=ol-41-6-1142

[82] M. Neuhaus *et al.*, "10 W CEP-stable few-cycle source at 2 m with 100 kHz repetition rate," *Opt. Express*, vol. 26, no. 13, pp. 16074–16085, Jun. 2018. [Online]. Available: https://www.osapublishing.org/abstract.cfm?URI=oe-26-13-16074

[83] H. Fattahi, *Third-Generation Femtosecond Technology* (ser. Springer Theses). Cham, Switzerland: Springer, 2015. [Online]. Available: 10.1007/978-3-319-20025-5

[84] H. Fattahi *et al.*, "Near-PHz-bandwidth, phase-stable continua generated from a Yb:YAG thin-disk amplifier," *Opt. Express*, vol. 24, no. 21, pp. 24337–24346, Oct. 2016. [Online]. Available: https://www.osapublishing.org/abstract.cfm?URI=oe-24-21-24337

[85] F. Tavella, A. Marcinkevičius, and F. Krausz, "Investigation of the superfluorescence and signal amplification in an ultra-broadband multiterawatt optical parametric chirped pulse amplifier system," *New J. Phys.*, vol. 8, no. 10, pp. 219–219, Oct. 2006. [Online]. Available: http://stacks.iop.org/1367-2630/8/i=10/a=219?key=crossref.c576587b6ce4fbaff676a545f9fbcb1a

[86] N. Ishii *et al.*, "Multimillijoule chirped parametric amplification of few-cycle pulses," *Opt. Lett.*, vol. 30, no. 5, pp. 567–569, Mar. 2005. [Online]. Available: http://ol.osa.org/abstract.cfm?URI=ol-30-5-567

[87] H. Telle *et al.*, "Carrier-envelope offset phase control: A novel concept for absolute optical frequency measurement and ultrashort pulse generation," *Appl. Phys. B*, vol. 69, no. 4, pp. 327–332, Feb. 2014. [Online]. Available: http://link.springer.com/10.1007/s003400050813

[88] C. Teisset *et al.*, "Soliton-based pump-seed synchronization for few-cycle OPCPA," *Opt. Express*, vol. 13, no. 17, pp. 6550–6557, 2005. [Online]. Available: http://www.mendeley.com/research/solitonbased-pumpseed-synchronization-for-fewcycle-opcpa/

[89] A. Schwarz *et al.*, "Active stabilization for optically synchronized optical parametric chirped pulse amplification," *Opt. Express*, vol. 20, no. 5, pp. 5557–5565, Feb. 2012. [Online]. Available: http://www.opticsexpress.org/abstract.cfm?URI=oe-20-5-5557

[90] H. Fattahi *et al.*, "Pump-seed synchronization for MHz repetition rate, high-power optical parametric chirped pulse amplification," *Opt. Express*, vol. 20, no. 9, pp. 9833–9840, 2012.

[91] S. Prinz *et al.*, "Active pump-seed-pulse synchronization for OPCPA with sub-2-fs residual timing jitter," *Opt. Express*, vol. 22, no. 25, pp. 31050–31056, Dec. 2014. [Online]. Available: https://www.osapublishing.org/oe/abstract.cfm?uri=oe-22-25-31050

[92] H. Fattahi, H. Wang, A. Alismail, and F. Krausz, "Towards high-power, multi-TW light transients," in *Proc. Conf. Lasers Electro-Opt.*, Washington, DC, USA, 2016, Paper SM1M.6. [Online]. Available: https://www.osapublishing.org/abstract.cfm?URI=CLEO_SI-2016-SM1M.6

[93] H. Fattahi, "Sub-cycle light transients for attosecond, X-ray, four-dimensional imaging," *Contemporary Phys.*, vol. 57, no. 4, pp. 580–595, Oct. 2016. [Online]. Available: https://www.tandfonline.com/doi/full/10.1080/00107514.2016.1231870

[94] A.-L. Calendron, H. Çankaya, G. Cirmi, and F. X. Kärtner, "White-light generation with sub-ps pulses," *Opt. Express*, vol. 23, no. 11, pp. 13 866–13 879, Jun. 2015. [Online]. Available: https://www.osapublishing.org/oe/abstract.cfm?uri=oe-23-11-13866

[95] T. Buberl, A. Alismail, H. Wang, N. Karpowicz, and H. Fattahi, "Self-compressed, spectral broadening of a Yb:YAG thin-disk amplifier," *Opt. Exp.*, vol. 24, no. 10, pp. 10286–10294, May 2016. [Online]. Available: https://www.osapublishing.org/abstract.cfm?URI=oe-24-10-10286

[96] L. Indra *et al.*, "Picosecond pulse generated supercontinuum as a stable seed for OPCPA," *Opt. Lett.*, vol. 42, no. 4, pp. 843–846, Feb. 2017. [Online]. Available: https://www.osapublishing.org/abstract.cfm?URI=ol-42-4-843

[97] A. Alismail, H. Wang, N. Altwaijry, and H. Fattahi, "Carrier-envelope phase stable, 54 μJ, broadband, mid-infrared pulse generation from a 1-ps, Yb:YAG thin-disk laser," *Appl. Opt.*, vol. 56, no. 17, pp. 4990–4994, Jun. 2017. [Online]. Available: https://www.osapublishing.org/abstract.cfm?URI=ao-56-17-4990

[98] S.-W. Huang, J. Moses, and F. X. Kärtner, "Broadband noncollinear optical parametric amplification without angularly dispersed idler," *Opt. Lett.*, vol. 37, no. 14, pp. 2796–2798, 2012.

[99] H. Çankaya *et al.*, "40-J passively CEP-stable seed source for ytterbium-based high-energy optical waveform synthesizers," *Opt. Express*, vol. 24, no. 22, pp. 25169–25180, Oct. 2016. [Online]. Available: https://www.osapublishing.org/abstract.cfm?URI=oe-24-22-25169

[100] M. Cassataro *et al.*, "Generation of broadband mid-IR and UV light in gas-filled single-ring hollow-core PCF," *Opt. Express*, vol. 25, no. 7, pp. 7637–7644, Apr. 2017. [Online]. Available: https://www.osapublishing.org/abstract.cfm?URI=oe-25-7-7637

[101] M. Hentschel *et al.*, "Attosecond metrology," *Nature*, vol. 414, no. 6863, pp. 509–513, Nov. 2001. [Online]. Available: http://www.nature.com/doifinder/10.1038/35107000

[102] S. Keiber *et al.*, "Electro-optic sampling of near-infrared waveforms," *Nature Photon.*, vol. 10, no. 3, pp. 159–162, Jan. 2016. [Online]. Available: http://www.nature.com/doifinder/10.1038/nphoton.2015.269

[103] T. Amotchkina, H. Fattahi, Y. A. Pervak, M. Trubetskov, and V. Pervak, "Broadband beamsplitter for high intensity laser applications in the infra-red spectral range," *Opt. Express*, vol. 24, no. 15, pp. 16752–16759, Jul. 2016. [Online]. Available: https://www.osapublishing.org/abstract.cfm?URI=oe-24-15-16752

[104] A. Alismail *et al.*, "Near-infrared molecular fieldoscopy of water," in *Multiphoton Microscopy in the Biomedical Sciences XIX*, A. Periasamy, P. T. So, and K. König, Eds., vol. 10882. Bellingham, WA, USA: SPIE, Feb. 2019, p. 110. [Online]. Available: https://www.spiedigitallibrary.org/conference-proceedings-of-spie/10882/2507604/Near-infrared-molecular-fieldoscopy-of-water/10.1117/12.2507604.full

[105] R. E. Mainz *et al.*, "High-dynamic-range arrival time control for flexible, accurate and precise parametric sub-cycle waveform synthesis," *Opt. Express*, vol. 25, no. 4, pp. 3052–3068, Feb. 2017. [Online]. Available: https://www.osapublishing.org/abstract.cfm?URI=oe-25-4-3052

[106] T. Popmintchev *et al.*, "Bright coherent ultrahigh harmonics in the keV x-ray regime from mid-infrared femtosecond lasers," *Science*, vol. 336, no. 6086, pp. 1287–1291, Jun. 2012. [Online]. Available: http://www.ncbi.nlm.nih.gov/pubmed/22679093

[107] A. Gordon and F. X. Kärtner, "Scaling of keV HHG photon yield with drive wavelength," *Opt. Express*, vol. 13, no. 8, pp. 2941–2947, 2005. [Online]. Available: https://www.osapublishing.org/oe/abstract.cfm?uri=oe-13-8-2941

[108] A. Moulet, V. Tosa, and E. Goulielmakis, "Coherent kiloelectronvolt x-rays generated by subcycle optical drivers: A feasibility study," *Opt. Lett.*, vol. 39, no. 21, pp. 6189–6192, Oct. 2014. [Online]. Available: http://ol.osa.org/abstract.cfm?URI=ol-39-21-6189

[109] M. Wendl, M. Högner, and H. Fattahi, "Theoretical study: High harmonic generation by light transients," *Appl. Sci.*, vol. 8, no. 5, pp. 7281–7292, May 2018. [Online]. Available: http://www.mdpi.com/2076-3417/8/5/728

[110] S. Watanabe, K. Kondo, Y. Nabekawa, A. Sagisaka, and Y. Kobayashi, "Two-color phase control in tunneling ionization and harmonic generation by a strong laser field and its third harmonic," *Phys. Rev. Lett.*, vol. 73, no. 20, pp. 2692–2695, Nov. 1994. [Online]. Available: https://link.aps.org/doi/10.1103/PhysRevLett.73.2692

[111] P. Corkum, "Plasma perspective on strong field multiphoton ionization," *Phys. Rev. Lett.*, vol. 71, no. 13, pp. 1994–1997, Sep. 1993. [Online]. Available: http://link.aps.org/doi/10.1103/PhysRevLett.71.1994

[112] K. J. Schafer and K. C. Kulander, "High harmonic generation from ultrafast pump lasers," *Phys. Rev. Lett.*, vol. 78, no. 4, pp. 638–641, Jan. 1997. [Online]. Available: https://link.aps.org/doi/10.1103/PhysRevLett.78.638

[113] H. Wang, A. Alismail, G. Barbiero, M. Wendl, and H. Fattahi, "Cross-polarized, multi-octave supercontinuum generation," *Opt. Lett.*, vol. 42, no. 13, pp. 2595–2598, Jul. 2017. [Online]. Available: https://www.osapublishing.org/abstract.cfm?URI=ol-42-13-2595

[114] G. Arisholm, "General numerical methods for simulating second-order nonlinear interactions in birefringent media," *J. Opt. Soc. Am. B*, vol. 14, no. 10, pp. 2543–2549, Oct. 1997. [Online]. Available: http://josab.osa.org/abstract.cfm?URI=josab-14-10-2543

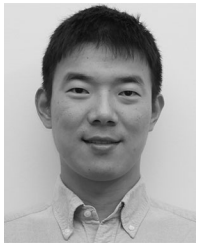

Haochuan Wang received the B.E. degree in optical engineering and the M.Sc. degree in optics from Zhejiang University, Hangzhou, China, in 2011 and 2014, respectively. He is currently working toward the Ph.D. degree with the Max-Planck-Institute for Quantum Optics, Munich, Germany, in the group of Prof. Dr. Ferenc Krausz. His research interests include supercontinuum generation, optical-parametric chirped-pulse amplification development, waveform synthesis, and femtosecond molecular fieldoscopy.

Ayman Alismail received the M.S. degree in nanotechnology and microsystems from Heriot-Watt University, Edinburgh, U.K. in 2011. He is currently working toward the Ph.D. degree in physics with Ludwig-Maximilians-University, Munich, Germany. In 2006, he joined the Physics and Astronomy Department, King Saud University, Riyadh, Saudi Arabia as a Lecturer, and in 2014 became a Reader. His current research interests include thin-disk lasers, chirped pulse amplification, spectral broadening, optical parametric amplification, waveform synthesis, overtone spectroscopy.

Gaia Barbiero received the bachelor's degree in physics and the master's degree in particle and applied physics, with a thesis on X-ray fluorescence, from Universita degli Studi di Milano - Bicocca, Milan, Italy, in 2013 and 2015, respectively. Since 2016, she has been working toward doctoral degree with the Department of Physics, Ludwigs-Maximilians University of Munich and Max-Planck-Institut of Quantumoptics. The main subject of her doctoral project is the development of a new broadband Stimulated Raman Spectroscopy tool for label-free spectroscopy.

Raja Naeem Ahmad received the bachelor's degree in applied physics from the University of Engineering and Technology, Lahore, Pakistan. He is currently working toward the master's degree with Ludwig Maximilians University of Munich, Garching, Germany. He was the recipient of Erasmus Mundas fellowship in 2015 and studied Materials Science at University of Torino, Italy. He is currently a research student with the Laboratory for Attosecond Physics, Max Plank Institute of Quantum Optics, Munich, Germany. His research interests include generation of ultrashort laser pulses and laser-based-spectroscopy.

Hanieh Fattahi studied applied physics at the Sharif University of Technology, Tehran, Iran, and the Ph.D. degree in physics from Ludwig Maximilians University of Munich, Munich, Germany. Since then, she has been a Researcher with the Laboratory for Attosecond Physics, Max Planck Institute of Quantum Optics, Garching, Germany. She is the recipient of the Minerva scholarship of Max Planck Society in 2016 and was elected as a member of Schiemann Kolleg in 2017. Her research centers on synthesis of intense controlled waveforms of laser light, design and development of thin-disk laser and OPAs, and femtosecond molecular fieldoscopy. She is the Fellow of Max Planck center for Extreme and Quantum Photonics in Ottawa, a visiting scientist with the Chemistry Department of Harvard University, and co-coordinator of the International Max-Planck Research School of Advanced Photon Science.